Volume 56
Number 58
25 July 2020
Pages 7987–8152

ChemComm

Chemical Communications

rsc.li/chemcomm

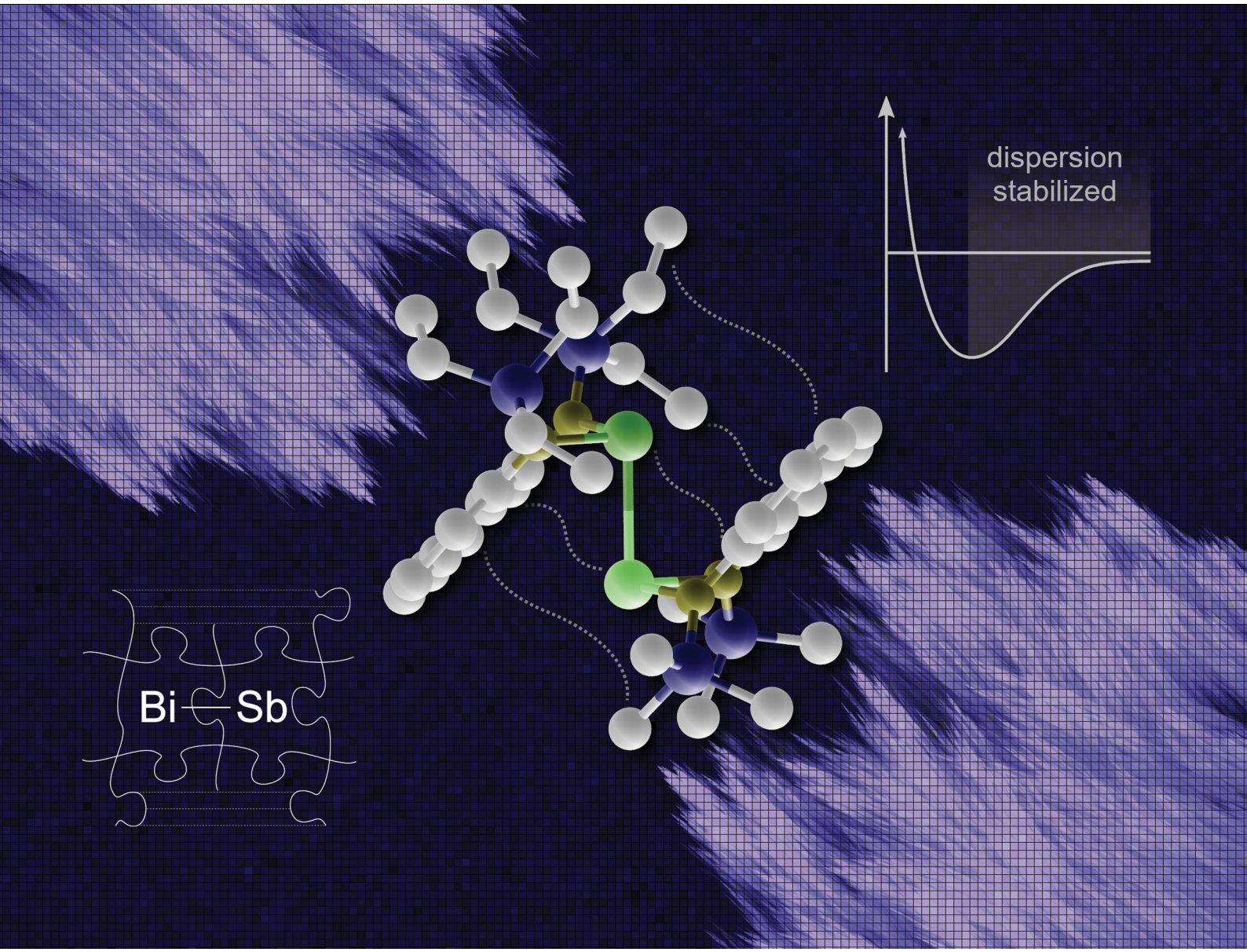

ISSN 1359-7345

ROYAL SOCIETY OF CHEMISTRY

COMMUNICATION

Katherine M. Marczenko and Saurabh S. Chitnis

Bismuthanylstibanes

ChemComm

COMMUNICATION

View Article Online
View Journal | View Issue

Check for updates

Cite this: *Chem. Commun.*, 2020, **56**, 8015

Received 10th January 2020,
Accepted 31st January 2020

DOI: 10.1039/d0cc00254b

rsc.li/chemcomm

Published on 03 February 2020. Downloaded on 5/1/2026 1:44:28 PM.

Bismuthanylstibanes†

Katherine M. Marczenko and Saurabh S. Chitnis *

Thermally-robust bismuthanylstibanes are prepared in a one-step, high yield reaction, providing the first examples of neutral Bi–Sb σ-bonds in the solid state. DFT calculations indicate that the bis(silylamino)naphthalene scaffold is well-suited for supporting otherwise labile bonds. The reaction chemistry of the Bi–Sb bond is debuted by showing fission using NH_3BH_3 and insertion of a sulfur atom, the latter providing the first example of a Bi–S–Sb motif.

Multiple bonding between heavy p-block elements (principle quantum number > 2) has been a topic of much research interest over the past several decades,[1–3] gradually eroding the perception that heavy elements do not form π bonds. Indeed, numerous compounds containing homonuclear or heteronuclear multiple bonds have now been obtained, revealing important theoretical insights and new reactivity paradigms.[1,2,4–6] Pursuing a program of developing new electronic structures and reactivity at Bi and Sb centres,[7–9] we were surprised to note that although a thermally robust Bi–Sb π-bond (*i.e.* RBi = SbR) has been known in an isolable compound for two decades (**A**, Scheme 1),[10] compounds containing the prototypical electron-precise σ-bond between these elements (*i.e.* $R_2Bi–SbR_2$, bismuthanylstibanes) have still not been isolated in the solid state. This is despite their presumed role as reaction intermediates[10,11] and their potentially valuable chemistry as single source precursors for deposition of BiSb,[12] which is a promising low-temperature n-type thermoelectric[13–15] and a topological insulator.[16,17]

This unusual gap is likely due to the kinetic lability of neutral Bi–Sb bonds – solution phase spectroscopic studies revealed that $Me_2BiSbMe_2$ undergoes rapid scrambling in solution to give combinations of dipnictanes at ambient temperature, precluding isolation of the heterobimetallic species.[18] The introduction of molecular charge has nevertheless enabled characterization of four charged compounds exhibiting Bi–Sb interactions (Scheme 1): the $[SbBi_3Br_9]^{3-}$ cluster anion (**B**),[19] the polymeric ribbon of $[BiSb_2]^{4-}$ (**C**) found in the network solid Ba_2BiSb_2,[20] and the molecular cations $[Ph_3SbBiCl_2]^+$ (**D**) and $[Ph_3SbBiCl]^{2+}$ (**E**).[21] These ions are likely persistent due to stabilization from lattice enthalpy and the high barrier to scrambling *via* associative interactions between similarly charged ions (coulombic repulsion). The successful isolation of these ionic examples encouraged us to seek the type of archetypal neutral σ-bond that is known for most element pairs in the p-block but remains as-yet unisolated between Bi and Sb centres.

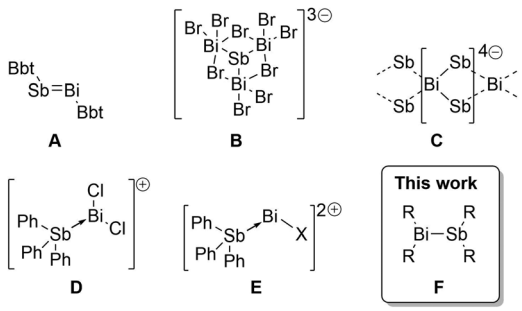

Scheme 1 Isolated compounds containing Bi–Sb bonds. See text for references. Bbt = *o*,*o*-$(CH(SiMe_3)_2)_2$-*p*-$C(SiMe_3)$-Ph.

Reactive functional groups at Bi and Sb centres have recently been stabilized using bulky and rigid bis(silylamino)naphthyl substituents.[8,22,23] Here we show that these substituents also provide access to persistent bismuthanylstibanes (**F** in Scheme 1), which contain the first structurally characterized neutral Bi–Sb σ-bonds. Contrary to previous examples, the Bi–Sb bonds reported here are remarkably stable against redistribution. Density functional theory (DFT) calculations ascribe this robustness to a combination of inductive and dispersive effects inherent to the bis(silylamino)-naphthalene scaffold. We also debut the reaction chemistry of the Bi–Sb functional group by revealing insertion of H^+/H^- and sulfur, evidencing, in the latter case, the first example of a Bi–S–Sb connectivity.

Attempts to form bismuthanylstibanes through traditional magnesium reduction or dehydrohalogenation reactions following

Department of Chemistry, Dalhousie University, 6274 Coburg Road, Halifax, Nova Scotia, B3H 4R2, Canada. E-mail: Saurabh.chitnis@dal.ca

† Electronic supplementary information (ESI) available: Detailed procedures and characterization data. CCDC 1975977–1975980 and 1980822. For ESI and crystallographic data in CIF or other electronic format see DOI: 10.1039/d0cc00254b

Published on 03 February 2020. Downloaded on 5/1/2026 1:44:28 PM.

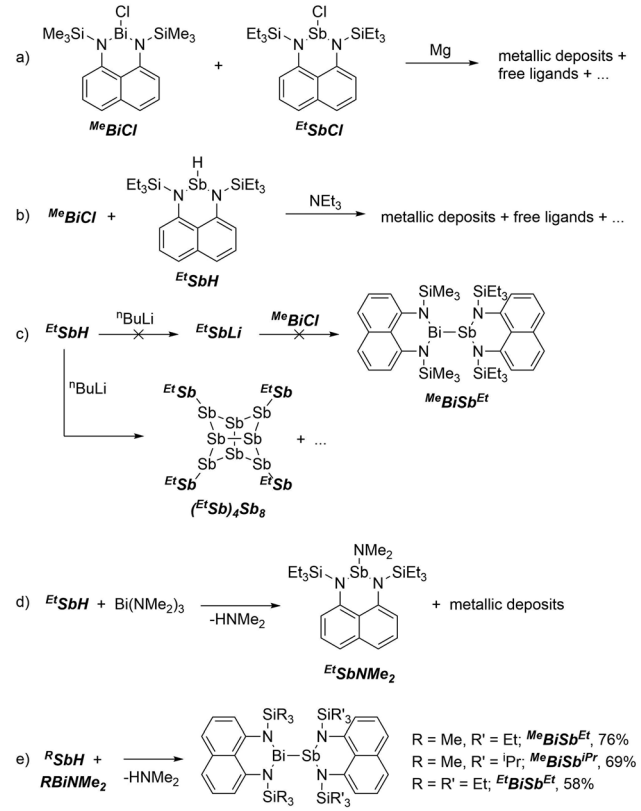

Scheme 2 Synthesis of $(^{Et}Sb)_4Sb_8$ and derivatives of $^{R}BiSb^{R'}$.

Tokitoh's route to BbtSb = BiBbt[10] were unsuccessful (Scheme 2a and b), yielding only intractable reaction mixtures containing metal deposits and traces of free ligands. We next envisioned the reaction of a preformed stibanide anion[24,25] with a chlorobismuthane (Scheme 2c) but these attempts were also foiled – instead of yielding the anticipated stibanide, deprotonation of ^{Et}SbH with ^{n}BuLi immediately gave a nearly insoluble red precipitate, which was identified by X-ray crystallography as the polystibane $(^{Et}Sb)_4Sb_8$. The asymmetric unit of this compound contains four ^{Et}Sb fragments connected by a tetracyclic Sb_8 cage (Fig. 1a). As this motif has previously been observed by Breuing[26] and Roesky,[27] we did not investigate the mechanism of its formation in further detail. An analogous structure featuring As–Sb bonds was also observed by Hänisch.[28]

Next we attempted deaminative coupling between ^{Et}SbH and $Bi(NMe_2)_3$ (at 0 °C and at −78 °C), which gave a light-yellow solution and a metallic precipitate (Scheme 2d). Analysis of the crude mixture by ^{1}H NMR spectroscopy showed formation of the antimony amide $^{Et}SbNMe_2$ (independently made from $^{Et}SbCl$ and $LiNMe_2$, Fig. S10, ESI†) and $HNMe_2$. We speculated that $^{Et}SbNMe_2$ could have formed *via* decomposition of a transient Bi–Sb bonded species by transfer of a NMe_2 group from Bi to Sb.

Consistent with this hypothesis, tethering the amino groups at both Bi and Sb suppressed such decomposition and finally yielded the targeted bismuthanylstibanes (Scheme 2e). Dropwise addition of ^{Et}SbH to $^{Me}BiNMe_2$ at −30 °C gave a dark red solution over a ten-minute period. Concentration of the reaction mixture gave bright red crystals of $^{Me}BiSb^{Et}$ in 76% isolated yield.

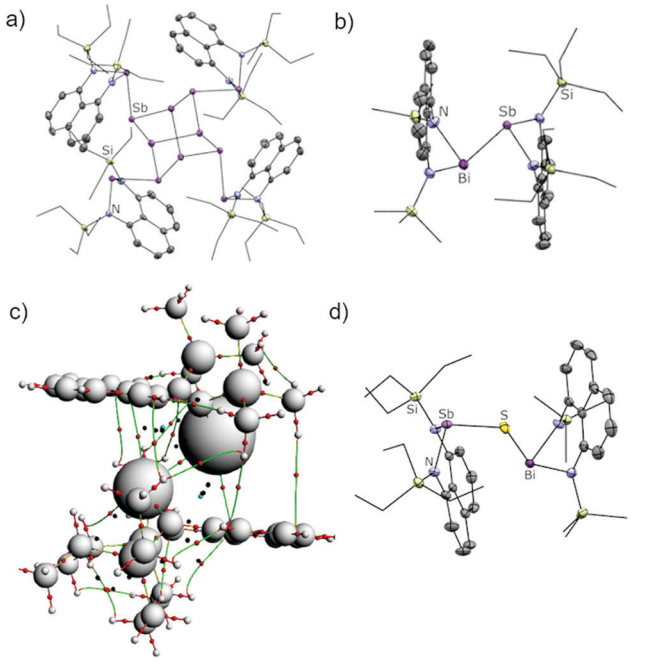

Fig. 1 (a) Single-crystal X-ray structures of $(^{Et}Sb)_4Sb_8$. (b) Single-crystal X-ray structures of $^{Me}BiSb^{Et}$. Selected bond lengths (Å) and angles (°): Bi–Sb 2.9775(9), Bi–N 2.161(4) and 2.161(4), Sb–N 2.059(4) and 2.059(4), N–Bi–N 83.6(2), N–Sb–N 87.6(2) (c) AIM calculated bond paths and critical points for $^{Me}BiSb^{Et}$. White spheres denote the nuclear basins (atoms). The vertical green lines evidence bonding interactions between the ligands in the periphery of the Bi–Sb bond. (d) Single-crystal X-ray structures of $^{Me}BiSb^{Et}$. Selected bond lengths (Å) and angles (°): Sb–S 2.3838(8), Bi–S 2.5456(7), Bi–N 2.141(2) and 2.150(2), Sb–N 2.040(2) and 2.045(2), N–Bi–N 83.86(8), N–Sb–N 89.35(8). Thermal ellipsoids are shown at the 50% probability level. Hydrogens have been omitted and silyl groups are shown in wireframe for clarity.

The silane substituents were easily varied through use of different precursors to give $^{Me}BiSb^{iPr}$ (69% isolated yield) and $^{Et}BiSb^{Et}$ (58% isolated yield). The reactions are quantitative by ^{1}H NMR spectroscopy and easily monitored by tracking the disappearance of the Sb–H resonance and formation of $HNMe_2$. Upon completion, the ^{1}H NMR spectra of bismuthanylstibanes show overlapping signals in the aromatic region due to the two distinct naphthalene diamine backbones (7.31–7.09 ppm). The alkyl region shows methylene, ethylene, and/or isopropyl signals with chemical shifts more upfield than the parent compounds.

The structures of all bismuthanylstibanes were confirmed by single-crystal X-ray diffraction (Fig. 1b and Fig. S1, ESI† for $^{Me}BiSb^{iPr}$ and $^{Et}BiSb^{Et}$). The asymmetric units contain a bimetallic structure with trigonal pyramidal antimony and bismuth atoms. The lone pair sites on each of the metallic atoms are oriented in opposite directions along the *a*-axis achieving maximum spatial distance between the two distinct naphthalenediamine ligand frameworks. Due to the similarity of the silyl groups present, a Bi/Sb substitutional disorder was detected in $^{Et}BiSb^{Et}$, rendering the crystallographic data suitable only for connectivity information. The Bi–Sb, Sb–N, and Bi–N bond lengths (see Fig. 1 caption and deposited CIFs) in $^{Me}BiSb^{Et}$ and $^{Me}BiSb^{iPr}$ do not significantly vary

 This journal is © The Royal Society of Chemistry 2020

Published on 03 February 2020. Downloaded on 5/1/2026 1:44:28 PM.

when the silane substituents are changed, indicating that this type of "outer sphere" bulk has little influence on the immediate bond parameters at the Bi–Sb bond. The N–Bi–N angle is slightly more contracted than the N–Sb–N angle in both cases (see Fig. 1 caption and deposited CIFs). The Bi–Sb bonds in $^{Me}BiSb^{Et}$ [2.9775(9) Å] and $^{Me}BiSb^{iPr}$ [2.9764(7) Å] is comparable in length to the value in TbtBi = SbTbt [2.972(5) Å], which is in line with the reduced bond order in heavy-atom formal double bonds.[6,29]

To assess the stability of the Bi–Sb bonds, a sealed sample of $^{Me}BiSb^{Et}$ was heated to 100 °C C_6D_6 for 72 h. No decomposition or redistribution was observed over this period, despite $^{Me}BiBi^{Me}$ and $^{Et}SbSb^{Et}$ being isolable compounds,[8,22] in contrast to the aforementioned facile redistribution involving alkyl/aryl-substituted Bi–Sb bonds.[18] To explore the specific influence of the bis(silylamino)naphthalene framework, we performed DFT calculations on $^{Me}BiSb^{Et}$, $Ph_2BiSbPh_2$, and $(Me_2N)_2BiSb(NMe_2)_2$. A Morokuma energy decomposition analysis (EDA)[30] revealed that the Bi–Sb bonding interaction in $^{Me}BiSb^{Et}$ (ΔE_{int} = −72.03 kcal mol^{-1}) is indeed intrinsically stronger than the corresponding interactions in the $Ph_2BiSbPh_2$ (ΔE_{int} = −52.55 kcal mol^{-1}) or $(Me_2N)_2BiSb(NMe_2)_2$ (ΔE_{int} = −46.72 kcal mol^{-1}).

As shown in Table 1, orbital (ΔE_{orb} values) and electrostatic (ΔE_{elstat} values) interactions are consistently more stabilizing in the amino-substituted compounds, because attachment to electronegative nitrogen atoms increases the partial charge (and therefore effective electronegativity) of the metal atoms. This lowers the energies of the interacting orbitals at the metals by inductive effects and simultaneously increases the extent of electrostatic bonding by making the metals stronger electron density acceptors. In particular, the rigid nature of the fused naphthalene backbone prevents effective overlap of the nitrogen lone pairs with the LUMO of the $^{Me}BiSb^{Et}$, further reducing electron density at the metal.[8] This view is supported by the more positive Natural Bond Orbital (NBO) derived partial charges at Bi and Sb (q_{Sb} and q_{Bi} values in Table 1) when the naphthalene framework is used compared to the values in $(Me_2N)_2BiSb(NMe_2)_2$, where free rotation around the metal-nitrogen bonds allows overlap of the nitrogen lone pairs with metal-centred acceptor orbitals. Attractive dispersion forces[31] between the bulky trialkylsilyl groups (known to be excellent dispersion donors)[32] also play a significant role in stabilizing $^{Me}BiSb^{Et}$ (ΔE_{disp} = −39.03 kcal mol^{-1}). Consistently, Bader's Atom-In-Molecules (AIM)[33] analysis detected numerous bond paths (Fig. 1c, vertical green lines) and bond critical points (red dots) between the ligands on each metal showing peripheral dispersive interactions between the bulky ligands. Thus, DFT calculations indicate that the bis(silylamino)naphthalene scaffold is uniquely suited to stabilize the otherwise weak Bi–Sb bond.

The reactivity of $^{Me}BiSb^{Et}$ towards a variety of unsaturated substrates was examined. No reaction between $^{Me}BiSb^{Et}$ and azobenzene, phenylacetylene, or pyridine *N*-oxide was observed after several days in the presence of UV light or in refluxing C_6D_6 (Scheme 3a). Photochemical or thermal scrambling to homonuclear species was also not observed at any point of these reactivity studies, emphasizing the stability of the Bi–Sb bond. Heating solutions of $^{Me}BiSb^{Et}$ and NH_3BH_3 resulted in fission of the metal–metal bond, giving ^{Et}SbH, borazine and a mixture of bis(trimethylsilylamino)naphthalene and bis(triethylsilylamino)naphthalene in a 10 : 2 ratio along with insoluble black metallic deposits (Scheme 2b). Based on the greater amount the trimethylsilyl-substituted ligand formed, we speculate that while ^{Et}SbH is a stable metal hydride,[8] transiently formed ^{Me}BiH is thermally unstable[34] and undergoes reductive elimination of bis(trimethylsilylamino)naphthalene and deposits metallic bismuth.

In contrast, clean insertion of a sulfur atom into the Bi–Sb bond was achieved by heating a solution of $^{Me}BiSb^{Et}$ and S_8 in toluene at 100 °C for 1 hour (Scheme 2c). The resulting compound, $^{Me}BiSSb^{Et}$, formed quantitatively by NMR analysis and isolated in 46% crystalline yield, contains the first example of the Sb–S–Bi connectivity. Notably, $^{Me}BiSSb^{Et}$ is also only the third structurally-characterized example of a molecular Sb–Z–Bi moiety, where Z is any element of the periodic table.[35,36] Compound $^{Me}BiSSb^{Et}$ was fully characterized and its structure

Table 1 Energy decomposition analysis for selected Bi–Sb bonded compounds at the BP86-D3/TZ2P level. The ΔE values are given in kcal mol^{-1}. ΔE_{int} (interaction energy) is the energy change upon Bi–Sb bond formation starting from fragments frozen in the geometry found in the bonded compound, while ΔE values includes relaxation of the fragments to their most stable free-molecule geometry. The difference between ΔE_{int} and ΔE is given by the ΔE_{prep} values. A doublet ground state was assumed for the fragments in all cases, indicating bond homolysis

Parameter	$^{Me}BiSb^{Et}$	$(Me_2N)_2BiSb(NMe_2)_2$	$Ph_2BiSbPh_2$
ΔE_{int}	−72.03	−46.72	−52.55
ΔE_{Pauli}	329.36	238.66	224.41
ΔE_{elstat}	−126.07	−88.05	−96.26
ΔE_{orb}	−236.29	−182.19	−159.15
ΔE_{disp}	−39.03	−15.14	−21.55
ΔE_{prep}	0.81	6.12	0.68
ΔE ($-D_e$)	−71.22	−40.60	−51.87
d/Å	3.003	2.981	2.940
q_{Sb}	1.15	0.92	0.64
q_{Bi}	1.12	0.93	0.68

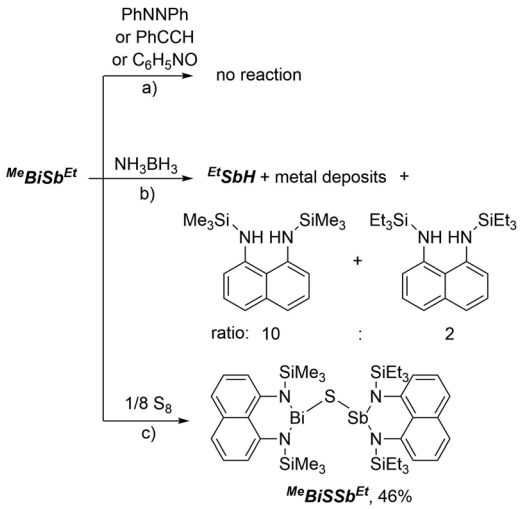

Scheme 3 Reactivity of $^{Me}BiSb^{Et}$.

Published on 03 February 2020. Downloaded on 5/1/2026 1:44:28 PM.

was determined crystallographically (Fig. 1d). The Sb–S [2.3838(8) Å] and Bi–S [2.5456(7) Å] bond lengths are within range of mean E–S bond lengths observed for antimony sulfides and bismuth sulfides (Sb–S: 2.527 ± 0.173 Å; Bi–S: 2.791 ± 0.177 Å) and the Sb–S–Bi angle [116.06(3)°] is as expected for a bent geometry at sulfur. The N–Bi–S bonding angles [91.52(6), 91.15(6)°] are significantly more contracted than the N–Sb–S angles [101.50(6), 102.49(6)°].

In summary, we have reported the synthesis of thermally-robust bismuthanylstibanes in a one-step, high-yield reaction, providing the first examples of neutral compounds with Bi–Sb σ-bonds. DFT calculations indicate that the bis(silylamino)-naphthalene scaffold is inherently well-suited for supporting otherwise labile bonds because it increases interaction energies through a combination of inductive effects and the dispersion donor effects. We also debuted the reaction chemistry of the Bi–Sb functional group by showing addition of H^+/H^- and insertion of a sulfur atom into the metal–metal bond. Further reactivity studies and the application of $^{R}BiSb^{R'}$ compounds as single-source precursors for depositing heterobimetallic phases are underway.

We acknowledge the Natural Sciences and Engineering Research Council (NSERC) of Canada, the Canada Foundation for Innovation (CFI), the Nova Scotia Research and Innovation Trust (NSRIT), and Dalhousie University for research funding. K. M. M. acknowledges the Vanier Canada Graduate Scholarships Program, the Killam Trusts, and the Walter C. Sumner Memorial Fellowships Program for funding. We thank Prof. Christian Hering-Junghans for valuable suggestions.

Conflicts of interest

There are no conflicts to declare.

Notes and references

1 E. Rivard and P. P. Power, *Inorg. Chem.*, 2007, **46**, 10047–10064.
2 P. P. Power, *Acc. Chem. Res.*, 2011, **44**, 627–637.
3 C. Präsang and D. Scheschkewitz, *Chem. Soc. Rev.*, 2016, **45**, 900–921.
4 R. C. Fischer and P. P. Power, *Chem. Rev.*, 2010, **110**, 3877–3923.
5 P. P. Power, *Nature*, 2010, **463**, 171–177.
6 H. B. Wedler, P. Wendelboe and P. P. Power, *Organometallics*, 2018, **37**, 2929–2936.
7 M. B. Kindervater, K. M. Marczenko, U. Werner-Zwanziger and S. S. Chitnis, *Angew. Chem., Int. Ed.*, 2019, **58**, 7850–7855.
8 K. M. Marczenko, J. A. Zurakowski, K. L. Bamford, J. W. M. MacMillan and S. S. Chitnis, *Angew. Chem., Int. Ed.*, 2019, **58**, 18096–18101.
9 K. M. Marczenko, J. A. Zurakowski, M. B. Kindervater, S. Jee, T. Hynes, N. Roberts, S. Park, U. Werner-Zwanziger, M. Lumsden, D. N. Langelaan and S. S. Chitnis, *Chem. – Eur. J.*, 2019, **25**, 16414–16424.
10 T. Sasamori, N. Takeda and N. Tokitoh, *Chem. Commun.*, 2000, 1353–1354.
11 T. Sasamori, N. Takeda and N. Tokitoh, *Phosphorus, Sulfur Silicon Relat. Elem.*, 2001, **169**, 89–92.
12 H. Zhang, J. S. Son, J. Jang, J.-S. Lee, W.-L. Ong, J. A. Malen and D. V. Talapin, *ACS Nano*, 2013, **7**, 10296–10306.
13 G. E. Smith and R. Wolfe, *J. Appl. Phys.*, 1962, **33**, 841–846.
14 W. M. Yim and A. Amith, *Solid-State Electron.*, 1972, **15**, 1141–1165.
15 B. Lenoir, A. Dauscher, M. Cassart, Y. I. Ravich and H. Scherrer, *J. Phys. Chem. Solids*, 1998, **59**, 129–134.
16 L. Fu and C. L. Kane, *Phys. Rev. B: Condens. Matter Mater. Phys.*, 2007, **76**, 045302.
17 D. Hsieh, D. Qian, L. Wray, Y. Xia, Y. S. Hor, R. J. Cava and M. Z. Hasan, *Nature*, 2008, **452**, 970–974.
18 A. J. Ashe, III and E. G. Ludwig, Jr., *J. Organomet. Chem.*, 1986, **303**, 197–204.
19 B. Wahl, L. Kloo and M. Ruck, *Angew. Chem., Int. Ed.*, 2008, **47**, 3932–3935.
20 S. Ponou and T. F. Fässler, *Inorg. Chem.*, 2004, **43**, 6124–6126.
21 E. Conrad, N. Burford, R. McDonald and M. J. Ferguson, *Chem. Commun.*, 2010, **46**, 4598–4600.
22 B. Nekoueishahraki, P. P. Samuel, H. W. Roesky, D. Stern, J. Matussek and D. Stalke, *Organometallics*, 2012, **31**, 6697–6703.
23 B. Nekoueishahraki, S. P. Sarish, H. W. Roesky, D. Stern, C. Schulzke and D. Stalke, *Angew. Chem., Int. Ed.*, 2009, **48**, 4517–4520.
24 H. J. Breunig, I. Ghesner, M. E. Ghesner and E. Lork, *Inorg. Chem.*, 2003, **42**, 1751–1757.
25 H. J. Breunig, M. E. Ghesner and E. Lork, *Z. Anorg. Allg. Chem.*, 2005, **631**, 851–856.
26 H. Breunig, R. Rosler and E. Lork, *Angew. Chem., Int. Ed. Engl.*, 1997, **36**, 2237–2238.
27 C. Schoo, S. Bestgen, A. Egeberg, S. Klementyeva, C. Feldmann, S. N. Konchenko and P. W. Roesky, *Angew. Chem., Int. Ed.*, 2018, **57**, 5912–5916.
28 D. Nikolova and C. von Hänisch, *Eur. J. Inorg. Chem.*, 2005, 378–382.
29 L. Zhao, S. Pan, N. Holzmann, P. Schwerdtfeger and G. Frenking, *Chem. Rev.*, 2019, **119**, 8781–8845.
30 K. Kitaura and K. Morokuma, *Int. J. Quantum Chem.*, 1976, **10**, 325–340.
31 J. P. Wagner and P. R. Schreiner, *Angew. Chem., Int. Ed.*, 2015, **54**, 12274–12296.
32 R. Pollice and P. Chen, *Angew. Chem., Int. Ed.*, 2019, **58**, 9758–9769.
33 R. F. W. Bader, *Chem. Rev.*, 1991, **91**, 893–928.
34 N. J. Hardman, B. Twamley and P. P. Power, *Angew. Chem., Int. Ed.*, 2000, **39**, 2771–2773.
35 A. Hinz, A. Schulz and A. Villinger, *Chem. Commun.*, 2015, **51**, 11437–11440.
36 C. Ritter, B. Ringler, F. Dankert, M. Conrad, F. Kraus and C. von Hänisch, *Dalton Trans.*, 2019, **48**, 5253–5262.

 This journal is © The Royal Society of Chemistry 2020